INVESTIGATION OF CLOUD PROPERTIES AND ATMOSPHERIC PROFILES WITH MODIS

SEMI-ANNUAL REPORT FOR JUL - DEC 1999

Paul Menzel, Steve Ackerman, Bryan Baum, Chris Moeller, Liam Gumley, Kathy Strabala, Richard Frey, Elaine Prins, Dan LaPorte, Xia Lin Ma and Tom Rink
CIMSS at the University of Wisconsin

Contract NAS5-31367

ABSTRACT

As the launch date of MODIS firmed up, final preparations were made for the processing, evaluation and quality assurance of the L1B and UW science data products. Minor additions were made to UW productions software; the means and methods of acquiring data needed for QA were identified. Visualization tools that will be used to display the final L1B and UW file formats are being developed. The UW SCF was augmented in anticipation of additional processing needs. MODIS direct broadcast hardware installation began, and initial L1B software neared completion. Science investigations progressed with the testing of simultaneous retrievals of atmospheric profiles and surface emissivity, the comparisons of HIRS cloud top properties retrievals with five years of ISCCP retrievals, and the good comparison of the UW global AVHRR cloud mask and the CLAVR retrievals. Finally, UW began making preparations for hosting the WISC-T2000 field experiment out of Truax field in Madison scheduled to begin mid February 2000.

TASK OBJECTIVES

Science Production Software Development

Small changes were made to the cloud mask and cloud top properties production software packages. The changes have been integrated into both the DAAC and MODAPS processing chains. Improvements to the clear radiance files used by both the cloud mask and cloud top properties code were started. Integration is expected sometime in March.

MODIS Infrared Calibration

UW began plans for MODIS data set collection to assess MODIS scan mirror Response versus Scan (RVS) using clear scenes of Antarctica. The data scenes will be cloud filtered using the MODIS Cloud Mask product (MOD35) and the clear scenes will be binned by Angle of Incidence (AOI). Average radiance as a function of AOI bin will define the RVS signal. In lieu of deploying a P-AERI instrument to Barrow, Alaska, a mobile AERI instrument housed in the UW Winnebago (i.e. the AERIbago) will be deployed at Madison, Wisconsin for measurements on frozen Lake Mendota in the February –March timeframe. This limited effort will test the concept of ground based measurements under MODIS on Terra for assessing MODIS performance.

WISC-T2000 Field Experiment

UW will host the WIsconsin Snow and Cloud experiment – Terra 2000 (WISC-T2000) beginning in mid February and extending through about mid March. A NASA ER-2 will be deployed to Madison, WI to pursue research in snow detection, clear atmosphere profiling, and cloud characterization during MODIS / Terra overpasses.

Cirrus Workshop

On October 28-29, 1999, Bryan Baum and the UW hosted a cirrus workshop for scientists to exchange information and opinions on the physical properties of cirrus clouds. Several action items resulted from the meeting; it is hoped these will be the foundation for future collaborations.

WORK ACCOMPLISHED

MODIS Production Software Development

Final pre-launch touches were added to the UW MODIS production software packages (cloud top properties, cloud phase, cloud mask and atmospheric profiles) during the last months of 1999. Additional error checking was added to the cloud mask (MOD35) processing to account for missing geolocation SDS's within the MOD03 product file. The MOD35 code will now return a first bit value of zero (no retrieval made) if the geolocation data is bad or missing for a given pixel.

Logic required to produce a calculated clear radiance value for every MODIS L3 grid box found to be clear was added to the cloud mask production software. The technique uses NCEP temperature and moisture profiles and a MODIS transmittance model to create a forward calculation of radiance for five MODIS IR bands. The forward model was generated by Hal Woolf (CIMSS/SSEC) using Terra IR spectral responses for each IR detector obtained from MCST. An average spectral response for each infrared band was computed. The band-averaged spectral response data were used to compute Planck coefficients and transmittances. The new transmittance model, along with the updated Planck functions were added to the UW MODIS shared code library. The MOD35 and MOD06 algorithms were updated to use the new routines.
(ftp://mcstftp.gsfc.nasa.gov/incoming/MCST/PFM_L1B_LUT_4-30-99).

In order to properly investigate relationships between the different atmosphere products derived from MODIS data, cloud top property results (cloud top pressure, temperature, emissivity) were separated into distinct day and night SDS's in the HDF-EOS product file (MOD06). These changes were also added to the Level 3 software by Paul Hubanks. This will allow all atmosphere products to be compared as daytime retrievals only.

Preparations for Launch

With the launch date of TERRA imminent as 1999 neared a close, UW began final preparations for gathering and distributing information about our products for our own use and for UW product users.

A cloud mask user's guide was written and posted on the web in PDF format. This guide contains basic information for MOD35 users in a succinct format; some of the information is not available from any of the other cloud mask documents (ie., ATBD). It can be accessed at http://cimss.ssec.wisc.edu/modis1/pdf/CMUSERSGUIDE.PDF

Thanks to Dr. Richard Buss at the GSFC DAAC, UW is now able to submit data subscriptions which automatically transfer selected MODIS products from the DAAC to the UW SCF for QA purposes. This process was complicated by the fact that there is no way to select the granules products based upon geographic location. We expect to select granules for the next day's investigation based upon any trouble locations we may identify in today's data.

UW personnel worked with some members of the land team to investigate cloud mask regions identified in the Land Team's QA Known Problems Page. Data from problem regions were ordered through MEBDOS and closely inspected. Each time, the cloud mask production software was found to be working as expected. The problem was either a result of bad synthetic data or with cloud mask thresholds that have been adjusted for AVHRR, HIRS and MAS data and may not be tuned for MODIS data yet. These discourses with our product users was invaluable and gave us a good indication of what to expect when our products become regularly available. A web page is being developed which will help users keep up with known cloud mask problems, solutions to the problems and code updates.

Effects of the Loss of 1.6 μm Data on the MODIS Cloud Mask for FM1

In November, UW was asked to assess the impact of the loss of 1.6 μm data on the MODIS cloud mask algorithm. This was in response to the possibility that more than half the channels of this band may be missing on FM1. Investigations indicated that the loss of 1.6 μm MODIS radiance data will affect the ability of the cloud mask to discern snow from cloud. A simple version of the Normalized Difference Snow Index (NDSI) is applied within the MODIS cloud mask algorithm to identify snow background scenes. If snow is found, the scene is most likely clear. In this way it serves to distinguish cloud from clear snow backgrounds. Loss of the 1.6 μm data without any other added snow information results in a decrease in the quality of the MODIS cloud mask product over snow covered regions. However, we believe this effect can be minimized and perhaps even mitigated through 1) the extrapolation of good 1.6 μm pixels, 2) the use of surrogate bands for snow detection and 3) the use of ancillary snow base maps.

1). Preparation for the launch of the Japanese Advanced Earth Observing Satellite II (ADEOS-II) and the Global Imager (GLI) led to an investigation of cloud and snow detection using an NDSI calculated with 1.6 and .55 μm bands of differing spatial

resolutions and sampling. The GLI will contain the 1.6 μm band at 250 m resolution sampled once within the 1 km footprint, while the .55 μm band will be at 1 km resolution. This concept of differing spatial resolutions is relevant to the 1.6 μm detector problem on the FM-1; the .55 μm 1 km aggregate channel can be used along with any good 1.6 μm pixels that fall within the 1 km footprint. The conclusion of the GLI investigation was that the use of 1.6 μm radiance data at sub-sampled 250 m resolution is warranted for snow detection in the GLI cloud mask. The overall percentages of snow/ice and cloud cover in the investigated MODIS Airborne Simulator (MAS) scenes were remarkably constant between the combined resolution and the 1 km resolution algorithms. There are problems associated with the combination of different spatial resolutions but they are found predominately in locations characterized by alternating open and forested areas and at snow cover boundaries and cloud edges. Scenes in such locations are difficult under the best conditions and using optimal data configurations.

2). Other techniques exist to separate snow from clouds. Baum and Trepte (1999) introduced a snow detection method utilizing a combination of .66, 11 and 3.7 μm bands. This method has been used in the University of Wisconsin real-time global cloud mask processing, the MODIS prototype. Comparisons between the NDSI and the Baum and Trepte technique using several MAS scenes generally show the NDSI to be more sensitive to snow detection (translating to finding more high confidence clear pixels). The percentage difference in clear sky translated in most scenes to less than 4 % per MAS flight track. This did vary from scene to scene due to background temperature (low signal to noise in the 3.7 μm channel over cold scenes) and viewing and solar geometry. An example of this comparison taken from a 12 February 1997 WINCE MAS data set is shown in Figure 1.

Another possibility would be to use the 2.1 μm band to improve snow detection. The MODIS snow and ice team will likely attempt to replace the 1.6 μm with the 2.1 μm band as part of the NDSI. UW will work with Dorothy Hall and George Riggs in testing this algorithm and its impact on snow and cloud detection.

3). Finally, some near-real time global snow and ice base maps produced from sources outside of MODIS are also available. The Near Real-Time SSM/I EASE-Grid Daily Global Ice Concentration and Snow Extent map produced at the NSIDC is used to identify snow backgrounds at night in the cloud mask processing. The limitations to these data sets are the rather course resolutions in which they are provided globally (22 km).

In summary, the loss of the 1.6 μm will affect the ability of the MODIS cloud mask to detect snow; however, we believe this effect can be alleviated through the use of extrapolation of good 1.6 μm pixels, the use of other snow detection techniques, and through the use of other sources of ice and snow coverage.

MODIS Visualization

Two separate MODIS visualization efforts are underway. MODIS L1B data in the revised file format can now be visualized and manipulated using the Man-computer Interactive Data Access System (McIDAS). This allows quick visual and computational comparisons of MODIS data with other surface and ground based instrumentation. The second effort is headed by Liam Gumley, who is creating IDL based tools to be used for visualization and analysis of the UW science products.

Direct Broadcast Hardware

In preparation for the installation of the EOS Direct Broadcast antenna, a tower was installed on the SSEC rooftop in November. In order to obtain the best possible view to the horizon (avoiding the existing geostationary satellite antennas), a 40-ft. tower was necessary. Consulting engineers Arnold and O'Sheridan conducted a structural analysis of the antenna/radome, tower, and building support structure to verify the integrity of the proposed installation, and to verify that the pointing accuracy of the antenna would be sufficient for reliable reception of X-band data. General contractors J.P. Cullen & Sons were contracted to assemble and install the tower. Due to the height and downtown location of the SSEC rooftop, the decision was made to use a helicopter to lift the tower sections to the roof. Industrial airlifting specialists Carson Helicopters were selected to provide the helicopter lift services. Following the installation of rooftop hardpoints anchored to the SSEC building frame, the tower was assembled in a parking lot adjacent to the SSEC building. On 27 November 1999, the helicopter lift took place. The roof support beams and tower sections were disassembled before the lift into 3 pieces, and each piece was lifted separately. The specially modified Sikorsky S-61 helicopter lifted the 3 sections to the roof within one hour. The installation of the antenna, radome, and associated processing hardware will take place in early March 2000. These efforts are being funded from other contracts but are reported here because of their relevance to the UW MODIS activities. See (*http://cimss.ssec.wisc.edu/~gumley/tower/xband.html*) for further information.

Direct Broadcast Software

Tom Rink joined the MODIS group to work on software development for direct broadcast processing. The goal was to port the operational MODIS L1A, geolocation, and L1B algorithms to a direct broadcast version, which removed some of the constraints of the operational versions. Requirements for the direct broadcast version were:

- Needs only the HDF toolkit to build,
- Must compile and run on SGI, Sun, IBM, and HP UNIX platforms,
- Must handle granule sizes other than 5 minutes,
- Multiple granules are not needed for calibration.

By the end of December, Rink had ported the L1A and geolocation codes in compliance with these requirements, and beta versions were distributed to external testers. The L1B code will be distributed to beta testers by the end of January 2000. These efforts are also being supported by other contracts.

UW Science Computing Facility (SCF)

The CIMSS MODIS SCF computing facility, a SGI Origin2000 system (16 CPUs, 4 GB RAM, 370 GB disk), was enhanced by the installation of an 18 kVA uninterruptible power supply (UPS). The UPS passed its first test on 1 January 2000 when a power outage in the early hours of the morning caused all other smaller SCF computers to reboot. The operating system on the Origin was updated to Irix 6.5.4, and all ECS toolkits were re-compiled as a result. A new IBM AIX system (RS/6000 43P 260) was acquired to replace an old existing system. This will be the primary McIDAS workstation for the MODIS group. A DLT-7000 tape drive was acquired along with this system to allow the new MAS digitizer DLT format to be read. A HP color laser printer and a HP color inkjet poster printer (36" format) were acquired to allow the MODIS group to produce the best possible MODIS graphical products.

MODIS Infrared Calibration

Preparation and planning for assessing MODIS in flight performance is underway. The MODIS PFM instrument on Terra was launched into orbit on 18 December 1999. Known performance issues associated with crosstalk and scan mirror reflectance will be closely monitored by UW. Plans for MODIS data set collection to assess these performance issues have been forwarded to MCST. UW is planning to obtain MODIS L1B data sets through the MODIS Atmosphere Group resources. A Large Data Sample (LDS) approach will be used to assess MODIS scan mirror Response versus Scan (RVS) using clear scenes of Antarctica. Antarctica is a desirable background to use for this assessment because of it's relatively flat scene radiance, the dry condition of the Antarctic atmosphere (esp. for high elevation), and the large number of daily MODIS observations (14 orbits per day). MODIS Band 31 will be evaluated first since it is devoid of PC band crosstalk, a complicating factor for other PC bands on PFM. The data scenes will be cloud filtered using the MODIS Cloud Mask product (MOD35) and the clear scenes will be binned by Angle of Incidence (AOI). Average radiance as a function of AOI will define the RVS signal. Resident natural variability in the MODIS data set will be assessed using AVHRR data scenes of Antarctica (AVHRR on NOAA15 will view the same region as MODIS on Terra, enabling collocation of AVHRR and MODIS data sets). The LDS approach will rely on obtaining a sufficient sample size so that natural variability is randomized over the various AOI. A small effect caused by snow surface emissivity dependence on view angle will be mitigated by comparing to AVHRR observations.

UW has decided not to deploy a P-AERI instrument to Barrow, Alaska in the March 2000 timeframe. Complications in transporting the P-AERI and support equipment from their current location in South Pole, Antactica to Barrow, Alaska had resulted in significant delays. In lieu of this, a mobile AERI instrument housed in the UW Winnebago (i.e. the AERIbago) will be deployed at Madison, Wisconsin for measurements on frozen Lake Mendota in the February –March timeframe. This limited effort will test the concept of ground based measurements under MODIS on Terra for assessing MODIS performance (as well as the thickness of the ice). In addition, a NASA ER-2 will be present to document scene variability of Lake Mendota during the AERIbago measurements.

An FM-1 Review meeting was held in Greenbelt, Maryland in August. Chris Moeller attended the meeting. Four primary performance issues of the FM-1 instrument were discussed: band to band registration between cold and warm focal planes, Analog to Digital Converter (ADC) anomalous performance (the "bin width" problem), band 23 and 32 responsivity changes, and duty cycle for the On Board Calibrator (OBC) and it's relationship to sector drift. It has been accepted that the OBC can be operated on a 30% duty cycle (as opposed to 100%) to avoid sector drift. This will prevent operating the OBC at it's design maximum temperature of about 315K (expected limit of about 300K with 30% duty cycle). The ADC anomolous performance (failure to output certain digital number values) appears related to the electronics configuration used by MODIS. Under the worst of these configurations, MODIS effectively loses 3 bits (becoming a 9 bit instrument). Configurations have been identified which do not cause ADC anomalies; however, restricting MODIS to these configurations limits the redundancy of the FM-1 instrument. Loss of redundancy is arguably a failure of the instrument, however, if the redundancy is never called upon during the lifetime of FM-1, there will be no impact. Band 23 and 32 responsivity decrease is troubling in that it may indicate a future failure. Between subsequent T/V cycles, the responsivity dropped about 5%. The behavior has not been explained but may be due to GSE setup (vignetting?). Cold and warm focal plane misalignment affects collocation of earth scene data for various MODIS bands. Within focal plane, the effect is small; however, for algorithms that use both cold and warm focal planes together (e.g. MODIS Cloud Mask), the effect is to cause an artificial signal gradient between bands on different focal planes. To test the effect of band to band registration (BBR) error, the MODIS cloud mask was run using simulated MODIS data (from MAS) of a partly cloudy region. The BBR error estimate from NASA was incorporated into the simulation. The results of this test showed that Cloud Mask outcome was changed about 5% of the time because of BBR error. The changed outcomes tended to cancel so that the summed cloud occurrence was within 1% of correct (See Figure 2).

ER-2 Activities

Plans are moving forward for the Wisconsin Snow and Cloud experiment – Terra 2000 (WISC-T2000). A NASA ER-2 will be deployed to Madison, Wisconsin (Truax Field) beginning in mid February and extending through about mid March. The ER-2 flights will pursue objectives in snow detection, clear atmosphere profiling and cloud characterization with the MODIS on Terra overhead. The data sets will be used to validate MODIS products including the MODIS Cloud Mask, Cloud Top properties, Top of Atmosphere Radiances, and Snow Mask. To accomplish this the ER-2 will carry the MAS, S-HIS, CLS and AirMISR instruments. MAS and S-HIS will provide the radiometric measurements to which MODIS science products can be compared, CLS will detect clouds and their heights in the ER-2 scenes, and AirMISR will be used to document reflectance characteristics of snow surfaces from multiple viewing angles. In addition to the MODIS based objectives, the ER-2 deployment will overlap with the ARM Cloud IOP 2000 activity starting about March 1. Coordination between the ER-2 and other aircraft (e.g. UND Citation for cloud in situ data) will be attempted. A large array of ground based instrumentation at the ARM CART SGP site will be overflown for

independent characterization of clear sky and clouds. About 10 ER-2 flights are anticipated, many near the overpass time (nominal 10:30 am local) of Terra. It is anticipated that MODIS will be operating in Science Mode (with Nadir Aperture Door open) during the entire ER-2 campaign.

A World Wide Web page is under construction for WISC-T2000.

DATA ANALYSIS

Atmospheric Profiles and Surface Emissivity Studies

Dr. Xia Lin Ma continued his efforts to improve the retrieval of surface temperature by combining the retrieval of atmospheric temperature and moisture profiles with the estimation of surface emissivity. His advancements included:

1) **Extension of the two-step physical retrieval algorithm**. The empirical orthogonal functions (EOFs) technique was applied to not only atmospheric temperature and humidity profiles but also to the surface emissivity spectrum. Thus, a surface emissivity spectrum (bands 30-50) is now retrieved along with an atmospheric temperature-humidity profile and surface skin temperature. It is being compared to seven band emissivities retrieved in the previous version.

2) **Testing of the extended version of the two-step physical algorithm using a global data set with a wide range of atmospheric and surface conditions.** A global subset of the NESDIS 1200 climatological database consisting of 117 profiles, which represent the range of meteorological conditions, was used as a training set for daytime regimes. A daytime data set was generated using a global subset with the following four parameter variations: a) surface skin temperature varies from surface air temperature Ta – 15 K to Ta + 15 K in steps of 3 K; b) local zenith angle varies from 0.0 (at nadir) to 20.0 degrees in steps of 5.0 degrees, from 20.0 to 42.0 degrees in steps of 2.0 degrees; c) solar zenith angle varies from 25.0 to 65.0 degrees in steps of 5.0 degrees; and d) the solar anisotropic factor varies from 0.85 to 1.15 in steps of 0.05. Atmospheric and surface property variations cover a wide range so that the data set covers all possible real situations. 1297296 profiles were generated. Surface elevation variation is temporarily not considered due to disc space limitations. A training nighttime data set was also constructed by using daytime temperature profiles linearly interpolated by -6 K at 1000 hPa and vapor mixing ratio profiles dried by 15% from 500-1000 hPa. A final test data set was selected from another NESDIS profiles subset consisting of 40 from three climatological zones (Middle-latitude, High-latitude and Tropical) and four seasons (Summer, Winter, Spring and Fall). The local zenith angle, solar zenith angle and solar anisotropic factor in the test data set were randomly generated. Surface emissivity data, consisting of band-averaged emissivities of 80 terrestrial materials, were randomly incorporated into the training and test data sets. The surface emissivity was allowed to vary between 0.56 to 0.99.

3) **Sensitivity and error analysis were conducted using the extended two-step physical retrieval algorithm:**

A) Errors due to solar anisotropic factor uncertainty

Currently there is no physical solar anisotropic factor (SAF) calculation model available. Therefore, SAF from a regression retrieval was used as a true value in the physical retrieval. Statistical results illustrate that there is no significant error increase in the physical retrieval when SAF uncertainty varies in a range of 5% RMS error (See columns 4 and 5 in Table 1).

B) Errors due to surface emissivity uncertainty

In the physical algorithm, it is assumed that surface band emissivities remain unchanged in the daytime and nighttime data sets. However, it is possible that some differences may exist due to surface moisture content change. When a random number with STD = 0.01 and Mean = 0. was added to the nighttime surface band emissivities, the RMSE of the retrieved parameters are slightly worse. Statistical results are summarized in columns 4 and 7 in Table 1.

C) Errors due to calibration and other uncertainty

A random number with STD = 0.2 K and Mean = 0. K was added into the day/night MAS simulated brightness temperature data sets to account for sensor calibration errors and other errors, such as pixel registration offset between multi-temporal observations. It was found that the RMSE of the retrieved parameters are not significantly worse compared to the retrieved results without noise (See columns 4 and 6 in Table 1)

4) **Evaluating the effect of combining daytime and nighttime measurements in the retrieval**. An investigation was conducted to evaluate the differences in retrieving geophysical parameters using both daytime and nighttime data sets, a daytime data set or a nighttime data set alone. Statistical results are summarized in Table 2. The following conclusions were drawn: a) retrieval accuracy of geophysical parameters from a combined day/night datasets is better than that from a daytime or a nighttime data set alone; b) the surface-reflected solar beam radiances provide essential information for the surface radiative property retrieval (emissivity/reflectivity). It is clearly evident that the retrieved surface emissivity accuracies are much poorer when using only night data.

5) **The retrieval source code was ported from a SUN platform to an SGI**.

6) **A case study using the WINTEX data sets is underway**. MAS flights 99-051 (track 7) and 99-055 (track 12) were selected as a daytime and a nighttime test data set in a winter regime. The extended physical retrieval algorithm is applied to MAS real observations to retrieve atmospheric temperature-humidity profile and surface properties simultaneously. Preliminary results have been obtained and await validation.

Global Cloud Mask from AVHRR (GCMA)

Testing of cloud masking techniques continued with the use of the GCMA (Global Cloud Mask from AVHRR), an automated daily, global cloud mask. AVHRR GAC (Global Area Coverage) data at 4 km resolution is analyzed for the presence of clouds using an algorithm similar to the MODIS cloud mask. The use of clear-sky radiance maps for land surfaces was implemented and tested. (The utility of these maps for nighttime water surfaces was previously established.) It was determined that these maps may aid in clear-sky determination particularly in arid and semiarid ecosystems, where application of the various threshold tests over bright surfaces and/or bare rock and soil sometimes leads to ambiguous results. However, no attempt will be made to incorporate these maps into MODIS processing until experience is gained with MODIS radiance measurements.

A comparison was performed between the GCMA and the CLAVR cloud masks. Fourteen consecutive orbits of AVHRR data from October 11, 1999 were used in the study. The comparison was limited to –60 to +60 degrees of latitude to avoid issues concerning radiance data quality and different ancillary information between the two methods (such as snow and ice cover). When considering the clear-sky fraction of all water scenes, the two methods compared well. However, GCMA found more clear skies in the daytime while CLAVR found more at night, especially in the subtropics. The daytime discrepancy was largely due to cases where GCMA found clear skies but CLAVR reported mixed (partly cloudy or mixed cloud types) conditions (almost 10% of total comparisons). When CLAVR mixed scenes and sun-glint areas were removed, the daytime values were very similar (Figure 3), but CLAVR still reported much more clear sky at night. For land cases, CLAVR consistently found more clear scenes than GCMA. When CLAVR mixed scenes were subtracted from these cases, the differences grew larger for both day and night cases.

Cloud data were collected over the southern African continent and adjacent oceans in anticipation of the SAFARI 2000 field campaign to be held in August and September 2000. Eleven years (1983-1993) of August and September stratus cloud and total cloud frequency data from ISCCP were analyzed. GCMA cloud frequencies were generated for September 1999 and compared to those of ISCCP. The two data sets compared very well over ocean regions; however; GCMA reported more clouds over central and eastern portions of the southern African land mass (Figure 4).

HIRS Cloud Climatology

Cloud statistics from the University of Wisconsin (UW) analysis of High resolution Infrared Sounder (HIRS) data were compared to the International Satellite Cloud Climatology Project (ISCCP) D2 statistics. The UW algorithm is the same one used to produce cloud top properties in MOD06. The comparison included monthly averages of frequency of total cloud cover, high clouds, and cloud properties (optical depths and IR emissivities) measured by each cloud detection system. The comparison focused on the months of January and July over five years. The UW HIRS analysis reported more total cloud cover and more high cloud cover than the ISCCP D2 in both January and July. The

ISCCP D2 detected clouds in 66-68% of their observations while the UW HIRS averaged 73-74%. The largest differences were in the ITCZ and the polar winter. For high clouds the ISCCP averaged 12% while the UW HIRS averaged 32%. The high cloud differences were greatest in the ITCZ – the largest being 29% for the ISCCP and 66% for UW HIRS at 10° N in July. Cloud radiometric properties were compared by converting the ISCCP visible optical depth measurements to equivalent infrared emissivities. The monthly averaged emissivities were similar – the ISCCP averages ranged from 76 to 79% while the UW HIRS were 68-69%. The largest cloud emissivity differences were in the ITCZ and the summer hemisphere.

This comparison uses a data set of five years from 1989 to 1993. Results covering five Julys from 1989-93 and four Januarys from 1990-93 are presented. The ISCCP D2 monthly averages were obtained from http://isccp.giss.nasa.gov/dataview.html. The ISCCP Total Cloud Amount (%), High Cloud Amount (%), and Optical Depth were compared to the UW HIRS monthly averages from the NOAA 10, 11, and 12 satellites. High Clouds are defined by the ISCCP as having pressure cloud top heights less than 440 mb.

The average frequencies of Total Cloud (also called All Clouds) and High Cloud detection reported by both the UW HIRS and ISCCP are shown in Figures 5 and 6. The UW HIRS and ISCCP Total Cloud detection generally agree at most latitudes. The exceptions occur in the tropics and the polar regions. The UW HIRS finds more of the thin cirrus in the tropics as noted by Jin et al. (1996). In the polar regions, the ISCCP finds more Total Cloud in the winter hemisphere while the UW HIRS reports more in the summer hemisphere.

There are two major differences in the cloud detection techniques that cause different reports of cloud frequency. First and foremost, the ISCCP uses solar reflectance data while the UW HIRS uses longwave infrared data. The increased cloud detection by ISCCP in the polar winters could be connected to a problem in correction for reduced solar illumination at low sun elevation angles. A second major difference is that the UW HIRS uses surface temperature data from NOAA for detecting clouds while the ISCCP does not. Jin et al. (1996) found that the UW HIRS reported fewer clouds than the ISCCP in high altitude mountains. This was attributed to a cold bias in the NOAA surface temperature analysis, which uses both conventional weather observations and satellite data. Satellite sea surface temperature data are available over oceans equatorward from 70° latitude, but not poleward from 70°. The UW HIRS cloud analysis thus has difficulty reliably detecting clouds in the polar regions and high altitude mountain ranges, such as the Himalyas and Andes, where there are few surface temperature data.

There are also several minor differences in the cloud detection techniques. One difference concerns how much colder a measured brightness temperature must be than the surface temperature to be labeled as a cloud. The ISCCP requires that a cloudy pixel be 4° C colder over land. This was reduced in the D series processing from the prior 6° C requirement of their C series, resulting in increased cloud detection. The UW HIRS uses a threshold of 2.5°, but the attenuation from water vapor in the 11 micron radiance

measurement is accommodated. The lower 2.5° C threshold for cloud detection in the UW HIRS system implies that more marginal pixels will be classified as clouds. Over land, the UW HIRS analysis guards against excessive cloud detection by using only the afternoon and sunset data from the NOAA satellites ignoring the night and sunrise data where the cold part of the diurnal cycle will cause false cloud reports. The diurnal cycle is most significant over land and does not create problems over oceans. An additional difference between the ISSCP and UW HIRS data sets is caused by differences in sensor resolutions. The imaging sensors used by the ISCCP have field of view (FOV) sizes of 5-8 km diameter. The HIRS is 19 km diameter in nadir (sub-spacecraft) views. Only nadir data have been used in this study. The larger FOV size can cause higher reports of clouds because small holes in broken cloud fields can not be detected. Wylie et al. (1994) estimates this error to be 2-3%.

Over all, the UW HIRS averaged 6-7% larger Total Cloud detection than the ISCCP (Table 3).

The High Cloud results also are shown in Figures 5 and 6, and Table 3. The UW HIRS is consistently higher than the ISCCP at mid- and tropical latitudes. The greatest differences occur in the Inter-tropical Convergence Zone (ITCZ) from 10° S to 10° N reaching 37%. The HIRS-ISCCP High Cloud detection difference averaged 20% over all latitudes (see Table 3). This difference is larger than previously reported by Jin et al. (1996). One possible reason for an increase the HIRS-ISCCP difference is a change in the monthly averaging of the UW HIRS data. The UW analysis was found to be very sensitive to sensor scan angle after the Jin et al. (1996) comparison was made. The data used in the Jin study have since been adjusted by 3% (increased frequency of cloud detection). Details of this correction are given in Wylie and Menzel (1999).

Cirrus Cloud Workshop

On October 28-29, 1999, Bryan Baum hosted a cirrus workshop at the UW to facilitate exchange of information and opinions on the physical properties of cirrus clouds. The primary focus of this workshop was the treatment of midlatitude cirrus, specifically the development of a multi-layer cirrus model and the sensitivity of visible and near-infrared reflectances to the assumption of cirrus habits. Some in-situ measurements of tropical cirrus were also presented .

Attendees: Bryan Baum and Yongxiang Hu (NASA LaRC); Andrew Heymsfield and Greg McFarquhar (NCAR); Robert Pincus, Ed Eloranta, Steve Ackerman, Kathy Strabala, Shaima Nasiri, Rich Frey, Steve Ackerman, Chris Moeller, Dan DeSlover, Erik Olson (AOS/SSEC/CIMSS – U. Wisc.); Paul Menzel and Jeff Key (NOAA); Ping Yang (NASA GSFC); Klaus Wyser (Stockholm Univ., Sweden)

Major conclusions from the workshop were the following:

1). Forward radiative transfer calculations indicate that visible and NIR reflectances are very sensitive to the assumption of habit and surface roughness. These calculations

should be extended to the 2- and 3-layer cirrus models now being developed. A more comprehensive suite of sensitivity studies should be performed from the visible through the infrared wavelength spectrum.

2). In-situ measurements of tropical cirrus are quite different from those of mid-latitude cirrus. Tropical cirrus have much larger aggregate cirrus particles even in the uppermost regions of the anvil cloud. Some thought should be given to separating cirrus generated from large-scale lifting processes from that formed by deep convection in satellite data.

3). Future development of a cirrus retrieval approach for interferometer data would be advantageous.

4). The group needs to tie in more with lidar/radar groups for validation.

5). Further exploration is needed of the weighting function concept for the visible and NIR channels.

Several action items also arose from the meeting:

1). Group: The group felt it was a good idea to come up with more of a group effort to win proposals, such as for the upcoming CRYSTAL Announcement of Opportunity. There was also discussion about a workshop recommendation for the SGP ARM CART site IOP this coming spring (2000). We would like a plane carrying the microphysical probes to make spirals through a cirrus cloud with an ER-2 overfly to get MAS, CLS (cloud lidar system) and interferometer data.

2). UW: The attendees at the workshop encouraged that more sensitivity studies be performed regarding individual crystal habits, smooth versus roughened particles, and multi-layer cirrus models. A set of WWW pages will be developed to help organize some of the newer results. Also suggested was the development of a multi-spectral technique to try to separate thin cirrus from the cirrus generated from deep convection. The main new efforts suggested were to (a) think of a way to most efficiently transfer new ideas into operational code, and (b) develop a procedure to retrieve cirrus properties from interferometer data.

3). NCAR: Action items include (a) list instruments and measured properties, (b) put more data on their web pages, especially for tropical and polar cases, (c) begin organizing data for some polar studies (coordinate with Jeff Key), (d) focus on a case study with Scanning HIS at Kwajalein Island, and (d) explore ways to best represent aggregates with multiple centers of mass.

4). GSFC (Ping Yang)/LaRC (Yong Hu): Intercompare DISORT and adding-doubling codes to determine source of discrepancies in results between the two approaches. Also extend comparison to a case involving an ice phase function. Investigate the issue of errors that may be incurred from truncating complex phase functions for use in the radiative transfer models.

5). GSFC (Ping): Generate scattering properties for the 1.6 um channel so that a sensitivity study, similar to that performed for smooth habits, can be completed. So far the UW has scattering properties for the visible and 2.1 um channel only. Also, develop scattering properties for spheroids and aggregates with multiple centers of mass, and more complete libraries for use in the 8-15 um spectrum for use with the interferometer and imager data. Complete initial studies on cirrus vertical inhomogeneity.

Another meeting was suggested for April 2000.

MAS IR Calibration Studies

Chris Moeller and Dan LaPorte attended the MAS instrument meeting in October at GSFC in Greenbelt, Maryland. At the meeting, discussions were held on MAS reflectance and emissive band calibration, L1B processing, and future instrument improvements and usage. Several decisions were reached and actions assigned during the meeting, including the use of JPL MAS BB emissivity estimates in future L1B processing, a resolution to characterize the MAS scan mirror performance, acceptance of the FTIR based measurements for characterizing MAS spectral response operationally, improved characterization of MAS BB emissivity through direct measurements by JPL and the addition of new thermistors to the blackbody surface, standardizing the timecode in MAS L1B files, and other items. Improvements to MAS, including new dichroics, redesigned dewar mounts, the implementation of a hard disk based recording system for inflight data, replacement/redesign of dewar pressure relief valves, and the ongoing investigation into the underperforming LVF for Port 3 were all discussed. In general, the performance of the MAS instrument is better monitored and understood than at any time in the past as we enter the post-launch phase of MODIS. The MAS team effort to maintain and improve the instrument is largely facilitated by this annual MAS instrument meeting.

For some time, MAS effective emissivity estimates (from system measurements of the Extended Area Blackbody, EABB) have demonstrated a minimum in effective emissivity moving towards long wavelengths near 14 microns. The nature of this minimum is a point of investigation. Direct reflectance measurements made at the JPL laboratory have not shown this behavior at 14 microns. Thus it seems likely that some other component of the MAS system measurements is responsible for this minimum in effective emissivity. To investigate this, laboratory measurements were made of the MAS BBs using the S-HIS instrument (April 1999) and of the EABB using S-HIS (July 1999). The purpose was to eliminate the MAS BB's and the EABB as the possible sources of the 14 micron effective emissivity minimum.

MAS blackbody emissivity and temperature reporting error have been investigated using April 1999 laboratory measurements of the MAS blackbodies. The S-HIS instrument was used to make the measurements. Of interest is the absolute emissivity of the MAS blackbodies as well as the spectral shape of the emissivity, particularly in the LWIR region where it has been postulated that emissivity is lower due to the thin nature of

Krylon paint coating on the blackbodies. By assessing the spectral shape of MAS BB emissivity, it will be possible to better understand the performance of other components of MAS (e.g. scan mirror, grating). S-HIS measurements were collected for MAS BB temperature settings of 14°C, 32°C, and 38°C for one blackbody (ambient inflight) and for 14°C, 32°C, 38°C, and ambient (about 22°C) for the 2nd blackbody (hot inflight). In all cases the MAS blackbodies were shrouded to minimize background effects during data collection. Background temperature and humidity were monitored with a probe. The S-HIS data were calibrated and scrutinized to identify periods of constant signal. The BB emissivity ε_{BB} is derived from the following:

$$\varepsilon_{BB} = \frac{L_{SHIS} - B(T_A)}{B(T_B) - B(T_A)} \qquad (1)$$

where L_{SHIS} is the S-HIS Planck radiance, $B(T_A)$ and $B(T_B)$ are the background and MAS BB Planck radiances respectively. The derived emissivity was convolved to MAS spectral response data to produce MAS broadband emissivity estimates. MAS BB emissivities (Figure 7) appear too high given knowledge of the BB coating and it's design; however, an important conclusion may be drawn from the relative spectral shape of the emissivity. There is no depression of emissivity near 14 microns. This finding refutes the hypothesis that the MAS BB coating is optically thin (which would allow reflectance by the underlying copper plate) at 14 microns. Importantly, this suggests that some other component (e.g. scan mirror, EABB, grating) of the MAS system measurements of the EABB is responsible for low effective emissivity estimates in that setup. A second conclusion of this test is that the MAS BB temperature reporting error may have a systematic bias. The emissivity determination is highly sensitive to temperature reporting error of the MAS BB (the $B(T_B)$ term in equation 1). A comparison of S-HIS observations and the reported BB temperature (thermistor readout) shows a decreasing bias moving towards higher MAS BB temperatures (Figure 8). This can be interpreted as a BB thermistor calibration error; however, further investigation is needed to validate this hypothesis.

The second test conducted was to ascertain if the EABB emissivity could be responsible for the minimum in MAS effective emissivity. Using laboratory measurements by S-HIS of a shrouded EABB (July 1999), the spectral shape of the EABB emissivity was evaluated. The objective of these measurements was to eliminate the EABB as the source of a deficit in the 14um derived blackbody effective emissivity (from MAS measurements of the EABB). Data analysis was possible for the EABB setting of 38°C. Data collection at higher EABB temperatures failed. The emissivity retrieval demonstrates that the EABB spectral emissivity is uniform across the LWIR region (Figure 9); this removes the EABB as a possible source of the 14um effective emissivity minimum previously deduced from MAS observations of the EABB. This, coupled with derived MAS BB emissivity from S-HIS measurements, suggests that the MAS LWIR BB emissivity is high and uniform and suggests that other components (scan mirror, grating) are responsible for the low effective emissivity estimates of the MAS BB in the 14um region. Characterization of the MAS scan mirror should become a goal of ARC.

UW will collaborate with ARC to look for ways to evaluate the MAS scan mirror performance and explain anomolously high calibrated radiances in the LWIR region.

An investigation has been initiated into use of the SABER onboard blackbody calibration source design for MAS. The SABER calibrator was described at the Logan Calibration Conference in November. The SABER blackbody has the advantage that the geometrical design (a series of holes) increases infrared emissivity above that of the current MAS flat plate blackbody design, and allows for a reflectance band source within one or more of the cavities in the blackbody. Thus, it may potentially provide both an emissive and reflectance band inflight source. Additionally, the use of a tunable laser will be evaluated as an inflight spectral calibration monitor. The investigation will next look closely at the feasibility of mounting a SABER type blackbody in the MAS scan cavity. A good opportunity to investigate this will occur when MAS is in Madison for the WISC-T2000 deployment.

PAPERS

Baum, Bryan A., Peter F. Soulen, Kathleen I. Strabala, Michael D. King, Steven A. Ackerman, and W. Paul Menzel, 2000: Remote sensing of cloud properties using MODIS airborne simulator imagery during SUCCESS. II. Cloud thermodynamic Phase. Accepted for publication in the Journal of Geophysical Research.

Chung, Sunggi., Steven A. Ackerman, Paul F. van Delst, and W. Paul Menzel, 2000: Cloud characteristics inferred from model calculations compared to HIS measurements. Accepted with revisions by the Journal of Applied Meteorology.

Frey, Richard A., Bryan A. Baum, W. Paul Menzel, Steven A. Ackerman, Christopher C. Moeller, and J. D. Spinhirne, 1999: A comparison of cloud top heights computed from airborne LIDAR and MAS radiance data using CO_2-slicing. Journal of Geophysical Research, Vol. 104, No. D20, 24,547-24,555.

Ma, Xialin, Zhengming Wan, Christopher C. Moeller, W. Paul Menzel, Liam E. Gumley and Yulin Zhang, 2000: Retrieval of Geophysical Parameters from MODIS Measurements: Evaluation of a Two-Step Physical Algorithm, submitted to Applied Optics.

Ma, Xialin, Zhengming Wan, W. Paul Menzel, Christopher C. Moeller, Liam E. Gumley and Yulin Zhang, 2000: Retrieval of Geophysical Parameters from MODIS Measurements: Extension of a Two-Step Physical Algorithm, presented at the 80th AMS meeting, 9-14 January, 2000, Long Beach, California.

Plokhenko, Youri and W. Paul Menzel, 2000: The effects of surface reflection on estimating the vertical temperature – humidity distribution from the spectral IR measurements. Accepted after revisions by the Journal of Applied Meteorology.

Wan, Zhengming, Yulin Zhang, Xialin Ma, Michael D. King, Jeffery S. Myers, and Xiaowen Li, 1999: Vicarious calibration of the Moderate-Resolution Image Spectroradiometer Airborne Simulator thermal-infrared channels, Applied Optics, Vol. 38, No. 30, 6294-6306.

Prins, Elaine P. and J. Schmetz, 1999: Diurnal Active Fire Detection Using a Suite of International Geostationary Satellites, paper presented during the Committee on Earth Observation Satellites (CEOS) GOFC Forest Fire Monitoring and Mapping Workshop, 3-5 November, in Ispra, Italy.

Wylie, Donald P. and W. Paul Menzel, 2000: Comparison of University of Wisconsin HIRS and ISCCP D2 Cloud Studies. Submitted to Journal of Geophysical Research Letters.

MEETINGS

Chris Moeller attended the MODIS FM-1 Review held 17 August in Greenbelt, Maryland.

Chris Moeller and Liam Gumley attended the MAS Instrument meeting on 19-20 October in Greenbelt, Maryland.

Bryan Baum hosted a cirrus workshop at the UW on 28-29 October in Madison, Wisconsin.

Elain Prins presented a paper entitled "Diurnal Active Fire Detection Using a Suite of International Geostationary Satellites" at the Committee on Earth Observation Satellites (CEOS) GOFC Forest Fire Monitoring and Mapping Workshop, 3-5 November, in Ispra, Italy.

Dan LaPorte attended a meeting of the Characterization and Radiometric Calibration for Remote Sensing, Space Dynamics Laboratory, Utah State University on 9-11 November in Logan, Utah.

Paul Menzel and Steve Ackerman attended the MODIS Science Team Meeting on 16-17 November in Columbia, Maryland.

Dan LaPorte was present for the TERRA launch 18 December at Vandenburg, Air Force Base, California.

Table 1. Resultant RMSE values when a two-step physical algorithm is applied to an independent data set (day/night combined data, 440 profiles, guess Solar Anisotropic Factor (SAF), no noise and unvaried night emissivities versus true SAF, noise added and varied night emissivities).

	Independent data set	Regression rtvl.	Physical rtvl. (guess SAF, no noise, unvaried emis.)	Physical rtvl. (true SAF, no noise, unvaried emis.)	Physical rtvl. (guess SAF, noise added, unvaried emis.)	Physical rtvl. (guess, SAF, no noise, varied emis.)
Layer (hPa)	T (K)	T (K)	T (K)	T (K)	T (K)	T (K)
Daytime						
1 (50-200)	8.11	0.88	0.84	0.85	0.87	0.87
2 (200-400)	6.05	1.99	1.78	1.78	1.80	1.78
3 (400-600)	10.92	1.96	1.55	1.56	1.60	1.58
4 (600-800)	12.10	1.88	1.41	1.40	1.41	1.47
5 (800-1000)	13.89	2.66	2.43	2.43	2.45	2.45
Ts (K)	18.80	0.76	0.49	0.49	0.52	0.55
TPW (cm)	1.04	0.36	0.25	0.26	0.27	0.25
Nighttime						
1 (50-200)	8.11	0.88	0.82	0.82	0.89	0.99
2 (200-400)	6.05	1.99	1.75	1.75	1.80	1.76
3 (400-600)	10.92	1.96	1.51	1.51	1.54	1.54
4 (600-800)	12.09	1.86	1.33	1.33	1.37	1.46
5 (800-1000)	13.90	2.66	2.40	2.40	2.44	2.46
Ts (K)	18.03	0.73	0.41	0.41	0.45	0.48
TWP (cm)	0.96	0.31	0.23	0.23	0.24	0.25
ε_{30}	0.059	0.022	0.011	0.011	0.012	0.011
ε_{31}	0.064	0.025	0.010	0.009	0.011	0.011
ε_{32}	0.062	0.024	0.009	0.007	0.009	0.009
ε_{33}	0.062	0.025	0.008	0.007	0.009	0.009
ε_{34}	0.060	0.027	0.009	0.008	0.009	0.009
ε_{35}	0.056	0.026	0.012	0.011	0.012	0.013
ε_{36}	0.049	0.025	0.015	0.014	0.015	0.016
ε_{37}	0.046	0.024	0.015	0.015	0.016	0.017
ε_{38}	0.043	0.023	0.018	0.018	0.018	0.020
ε_{42}	0.043	0.016	0.013	0.010	0.012	0.015
ε_{44}	0.026	0.012	0.008	0.008	0.010	0.010
ε_{45}	0.022	0.011	0.008	0.008	0.009	0.010

Ts: Surface skin temperature.
TPW: Total precipitable water vapor.

Table 2. Resultant RMSE values when a two-step physical algorithm is applied to an independent data set (440 profiles, day/night combined data versus daytime or nighttime data only).

	Regression rtvl. (day/night)	Physical rtvl. (day/night)	Regression rtvl. (day only)	Physical rtvl. (day only)	Regression rtvl. (night only)	Physical rtvl. (night only)
Layer (hPa)	T(K)	T(K)	T(K)	T(K)	T(K)	T(K)
1 (50-200)	0.88	0.84	1.04	0.95	1.00	0.87
2 (200-400)	1.99	1.78	2.12	1.99	2.06	1.86
3 (400-600)	1.96	1.55	2.26	1.66	2.07	1.68
4 (600-800)	1.88	1.41	2.24	1.55	1.93	1.52
5 (800-1000)	2.66	2.43	2.98	2.75	3.07	2.84
Ts(K)	0.76	0.49	0.92	0.68	1.10	1.01
TPW(cm)	0.36	0.25	0.40	0.30	0.38	0.30
ε_{30}	0.022	0.011	0.022	0.013	0.043	0.045
ε_{31}	0.025	0.010	0.023	0.012	0.050	0.051
ε_{32}	0.024	0.009	0.023	0.011	0.050	0.048
ε_{33}	0.025	0.008	0.024	0.010	0.051	0.049
ε_{34}	0.027	0.009	0.025	0.010	0.051	0.051
ε_{35}	0.026	0.012	0.025	0.012	0.050	0.051
ε_{36}	0.025	0.015	0.024	0.015	0.044	0.046
ε_{37}	0.024	0.015	0.025	0.017	0.042	0.045
ε_{38}	0.023	0.018	0.024	0.020	0.038	0.043
ε_{42}	0.016	0.013	0.017	0.016	0.022	0.021
ε_{44}	0.012	0.008	0.013	0.010	0.018	0.016
ε_{45}	0.011	0.008	0.013	0.011	0.016	0.016

Ts: Surface skin temperature.
TPW: Total precipitable water vapor.

Table 3. Global averages of the Total (All) Cloud frequency and High Cloud Frequency, and UW CO_2 HIRS cloud climatology and the ISCCP. The differences in the last column are column one minus column two.

	HIRS	*ISCCP*	*Difference*
Total (All Clouds)			
January	74%	68%	+6
July	73	66	+7
High Clouds			
January	32%	12%	+20
July	32	12	+20

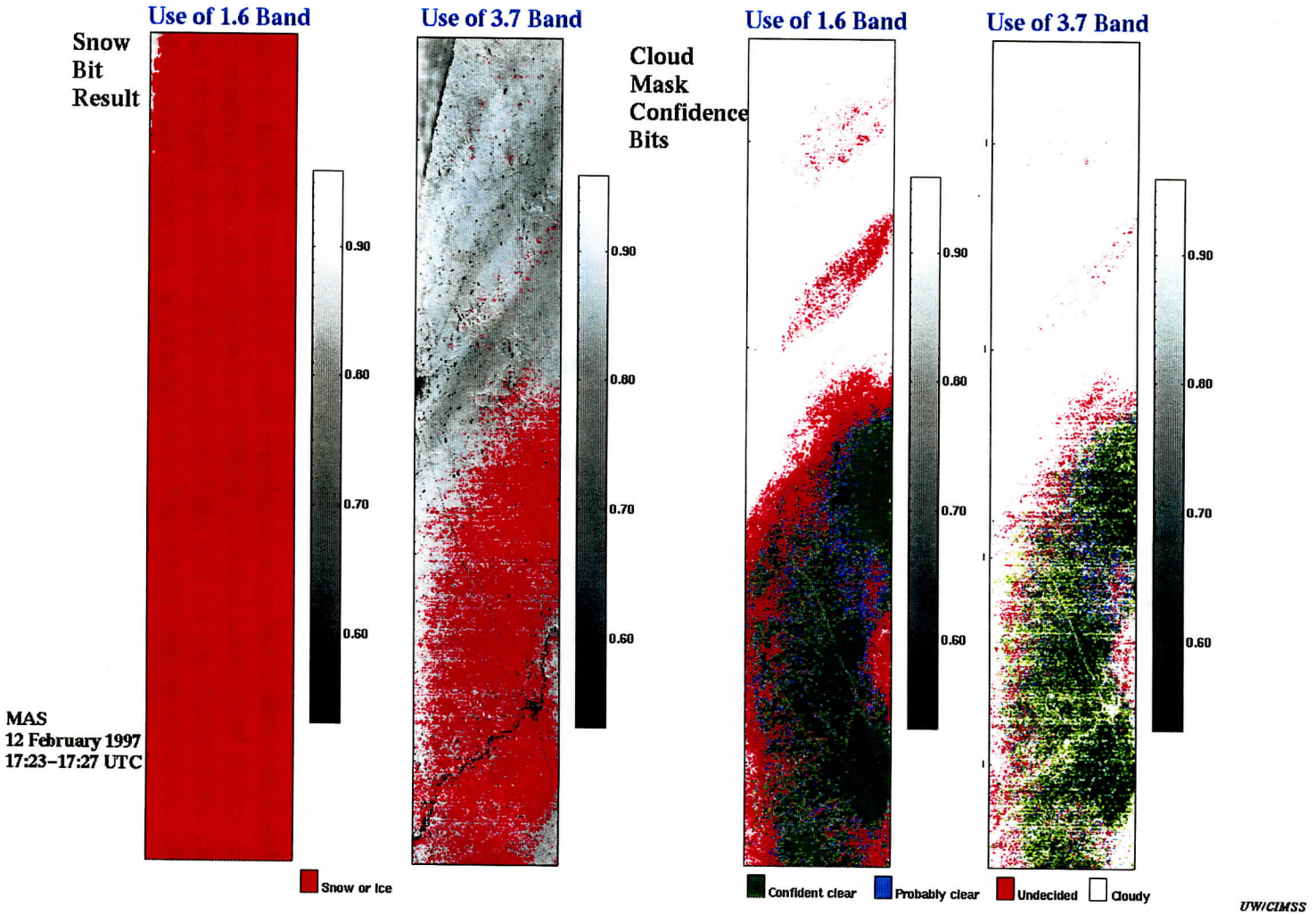

Figure 1. Example of the difference in cloud mask results when using the NDSI technique (first and third panels) and the 3.7 micron technique introduced by Baum and Trepte (1999) (second and fourth panels). The NDSI is the method currently implemented as part of the cloud mask production software.

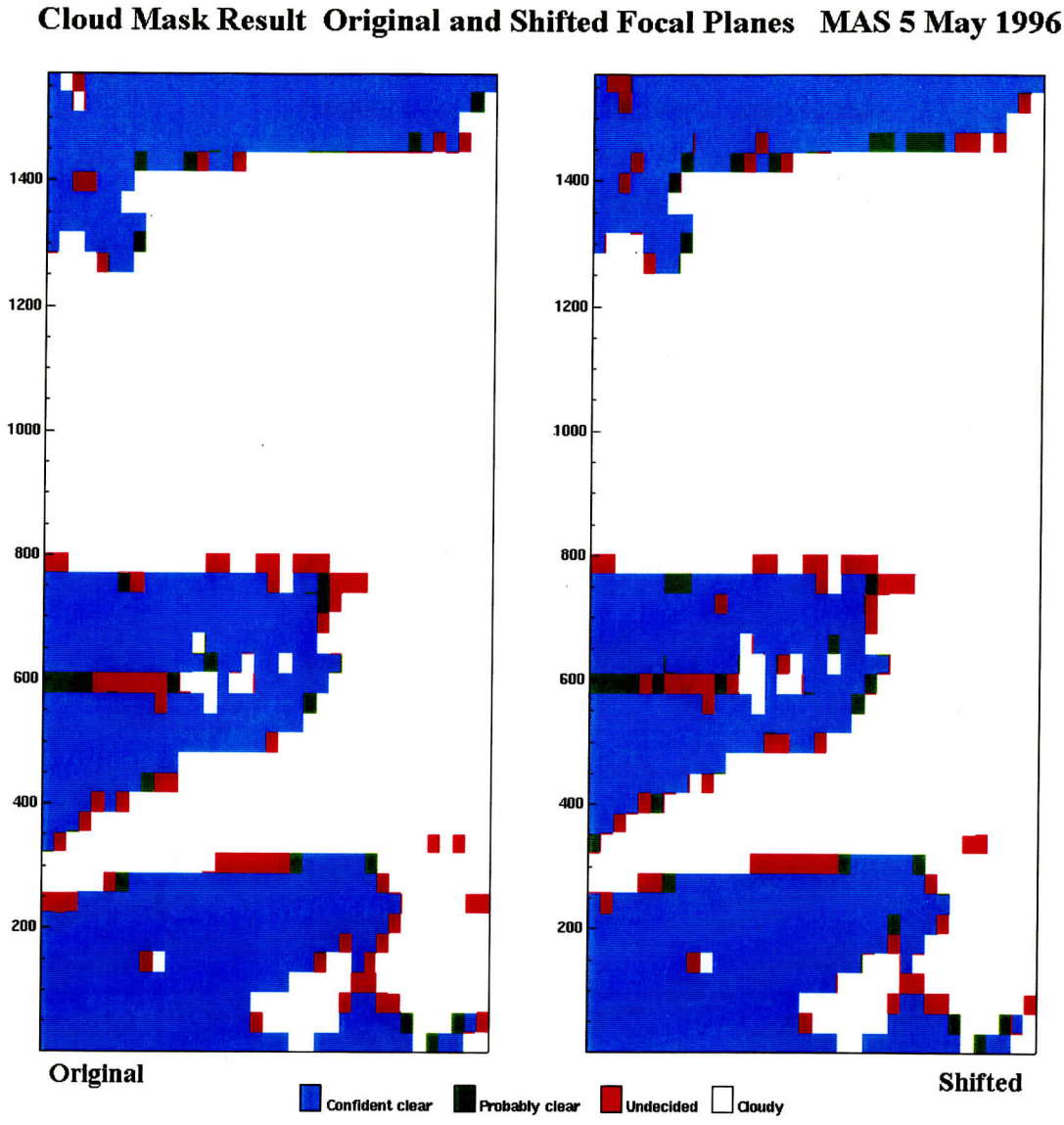

Figure 2. MODIS cloud mask result simulated using MAS data with Band to Band Registration (BBR) offset between MODIS cold and warm focal planes. Cloud Mask result changed about 5% of the time, resulting in a net 1% change in the cloud amount (cancellation occurred). In general, more "uncertain" results occurred. Uncertain Cloud Mask results are of questionable value to all (clear scene and cloudy scene) downstream MODIS Science Products because of the ambiguity of the cloud/no cloud determination.

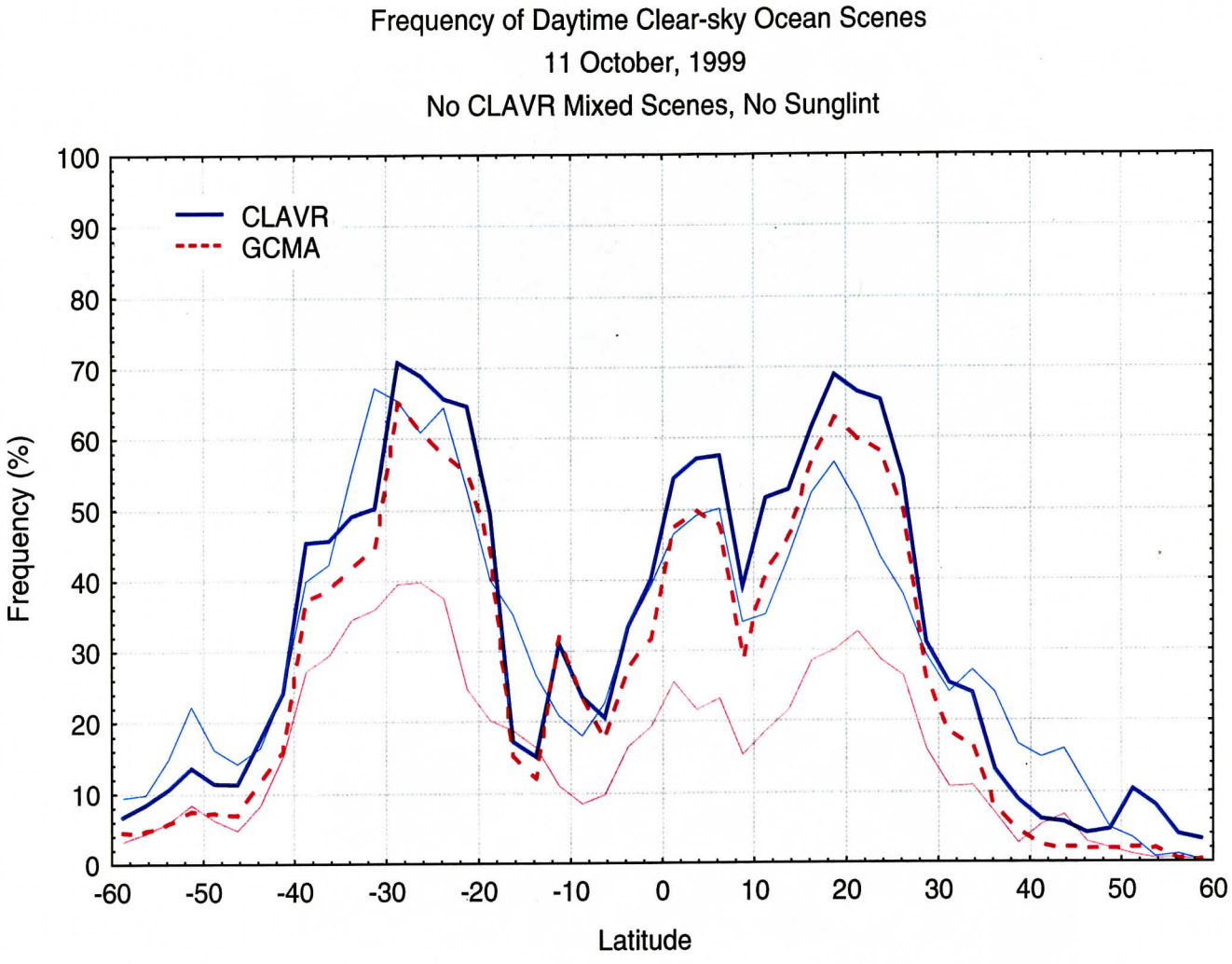

Figure 3. Frequency of daytime clear sky on 11 October 1999 determined by the UW Global Cloud Mask from AVHRR (GCMA) and CLAVR techniques using GAC data. The comparison consists of observations between -60 to + 60 degrees of latitude, no CLAVR mixed scenes and no sunglint regions. Under these conditions, the latitude trends in cloud detected between these two techniques is quite similar.

GCMA Total Cloud Frequency

September 1999

Cloud Frequency (%)

0 - 20 % Brown
20 - 30 % Tan
30 - 40 % Green
40 - 50 % Aqua
50 - 60 % Cyan
60 - 70 % Lt. Blue
70 - 80 % Dk. Blue
80 - 90 % Gray
90 - 100 % White

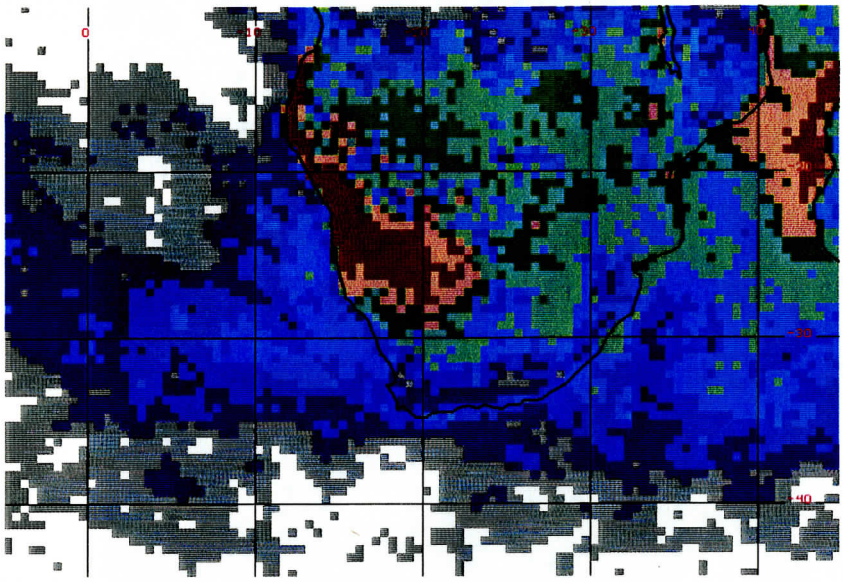

ISCCP Total Cloud Frequency

Combined August and September Means

Cloud Frequency (%)

10 - 20 % Brown
20 - 30 % Tan
30 - 40 % Green
40 - 50 % Aqua
50 - 60 % Cyan
60 - 70 % Lt. Blue
70 - 80 % Dk. Blue
80 - 90 % Gray
90 - 100 % White

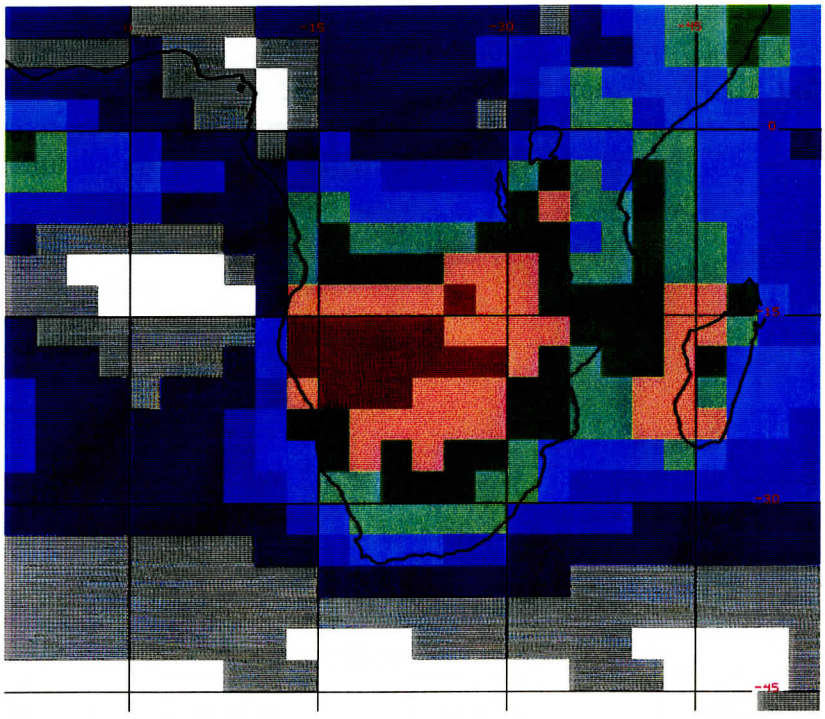

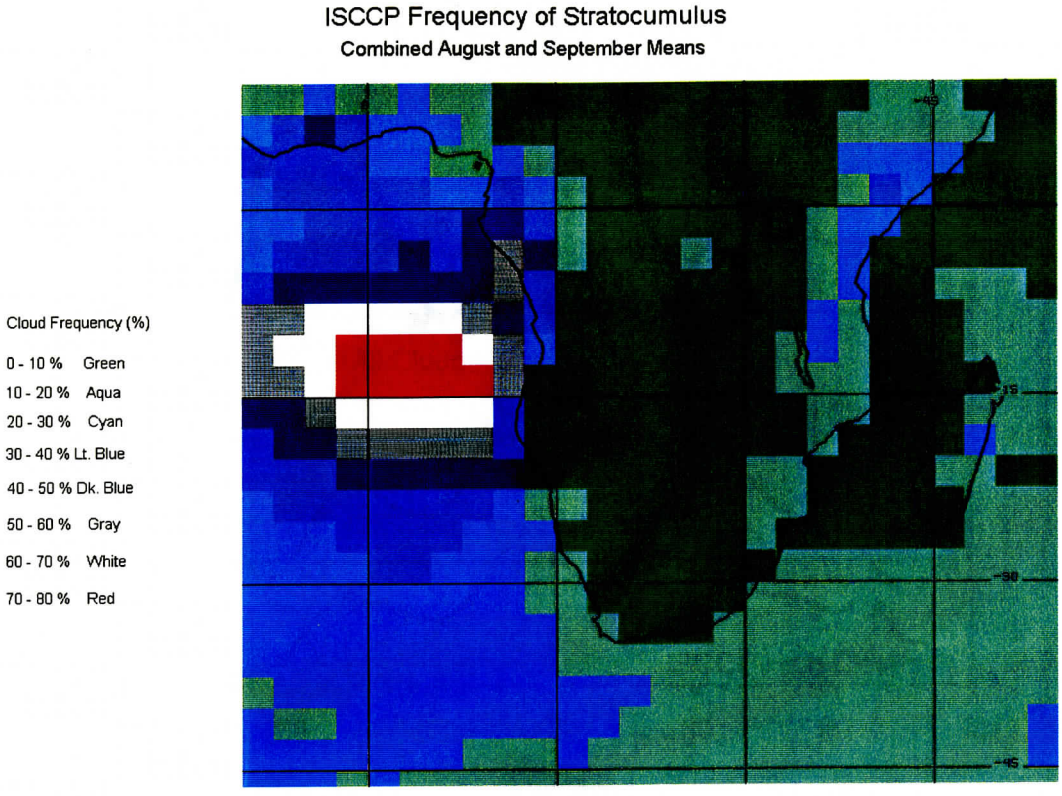

Figure 4. Total cloud frequencies for September 1999 from the GCMA (Global Cloud Mask from AVHRR) and for August and September combined from the ISCCP 11-year mean data set (top two figures, previous page). Bottom figure (this page) shows frequency of stratocumulus from the same ISCCP data set.

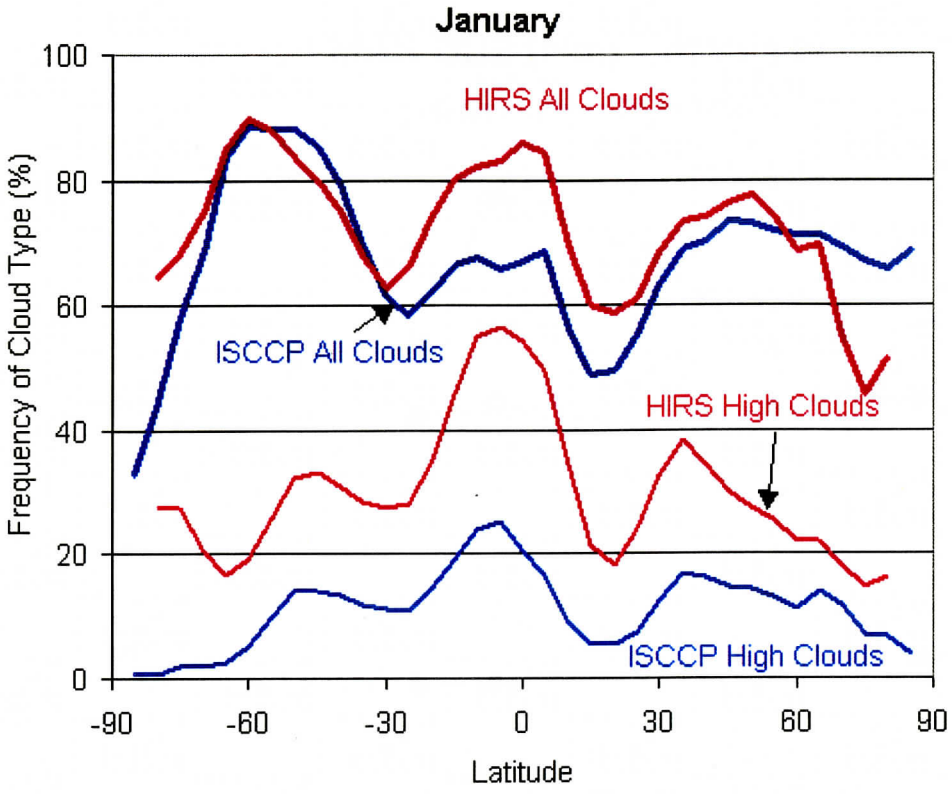

Figure 5. The frequency of detection of All Clouds (Total Cloud) and High Cloud (above 440 mb) for UW HIRS and ISCCP analyses; results from four Januarys in 90- 93.

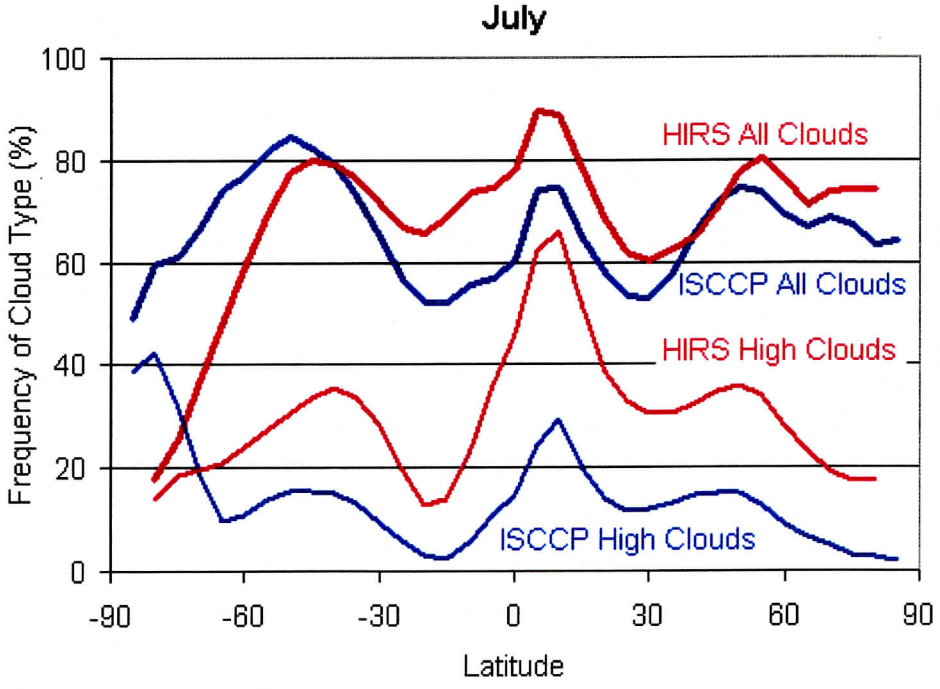

Figure 6. The frequencies of detection of All (Total) clouds and High clouds for five Julys from 1989-93.

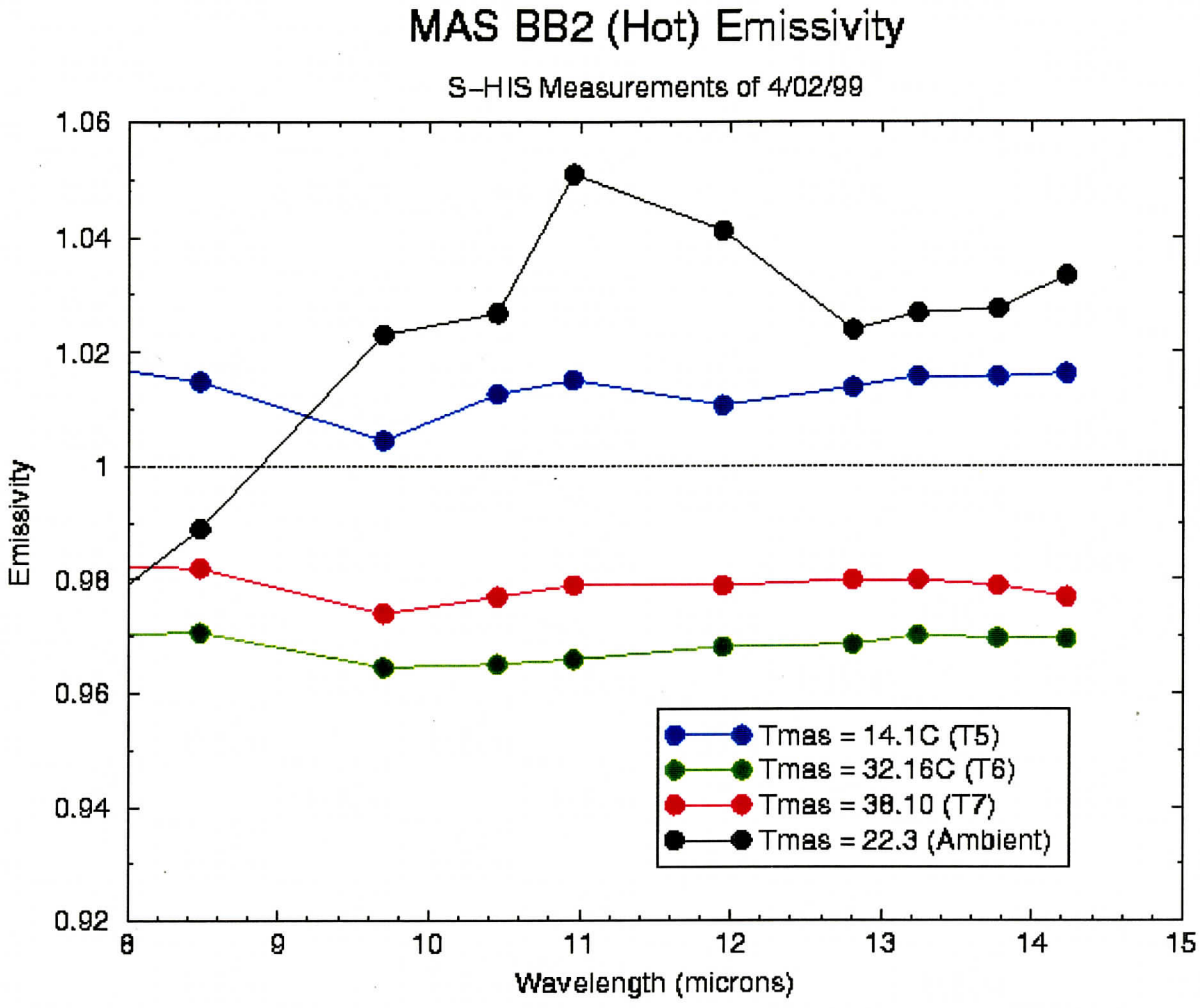

Figure 7. MAS blackbody emissivity determined from S-HIS laboratory measurements of April 1999. The most realistic emissivity retrievals are for MAS blackbody temperature settings of 32.16°C and 38.10°C. However, the sensitivity of the emissivity retrieval to MAS BB temperature reporting error makes it difficult to accept the absolute emissivity retrieval. Importantly, the relative spectral shape of the emissivity retrieval demonstrates that there is not an emissivity minimum near the 14um region. This has previously been observed in MAS system measurements but these results suggest that it is due to components other than the MAS blackbodies.

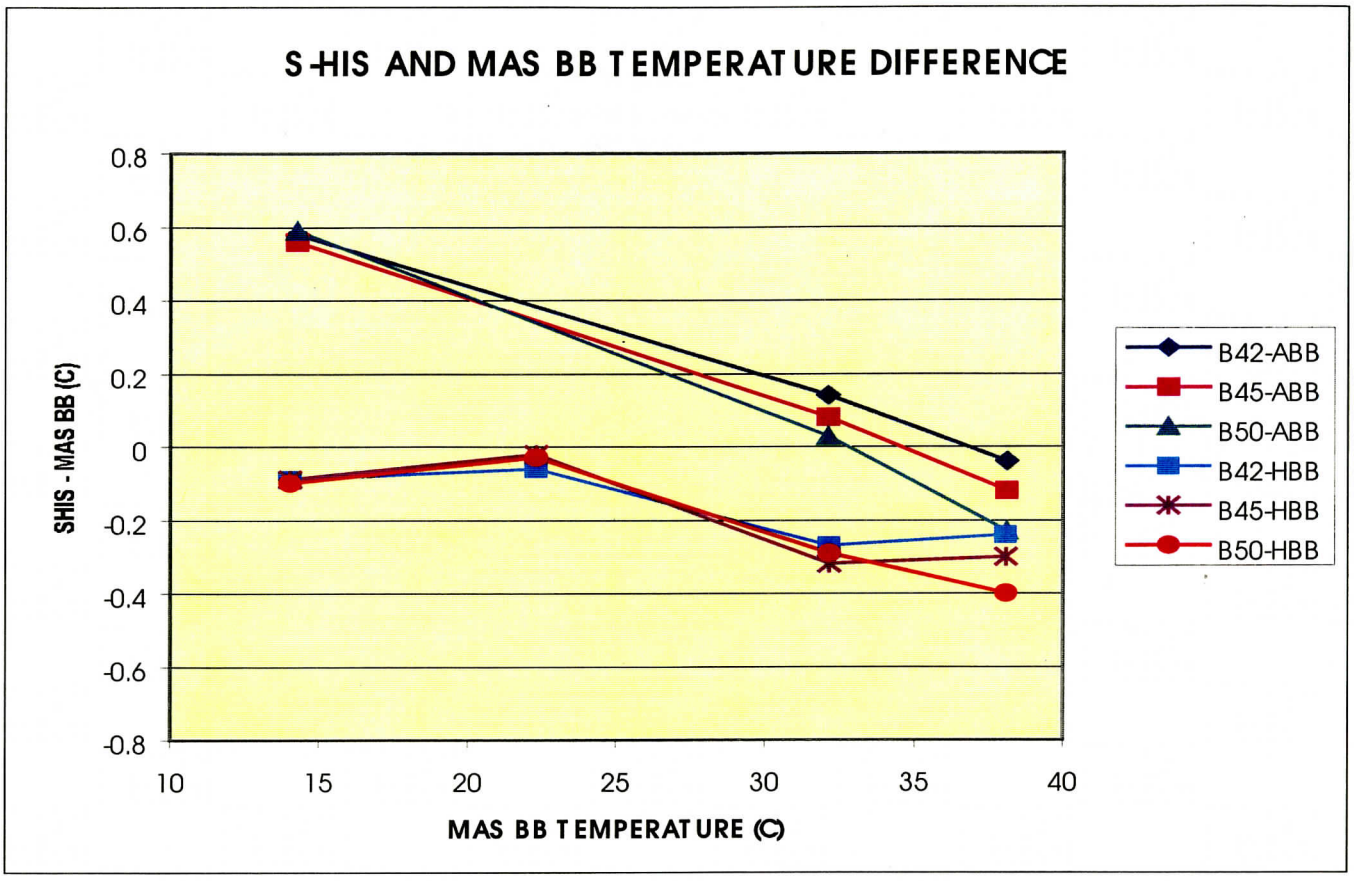

Figure 8. S-HIS brightness temperature minus MAS BB reported temperature for the MAS Ambient (ABB) and Hot (HBB) blackbodies (data set collected April 1999). The temperature difference is correlated to the MAS BB Temperature, especially for the ABB. This suggests that there is a temperature dependent MAS BB temperature reporting error in the ABB. This could be caused by a calibration error in the temperature reporting thermistor attached to the ABB plate.

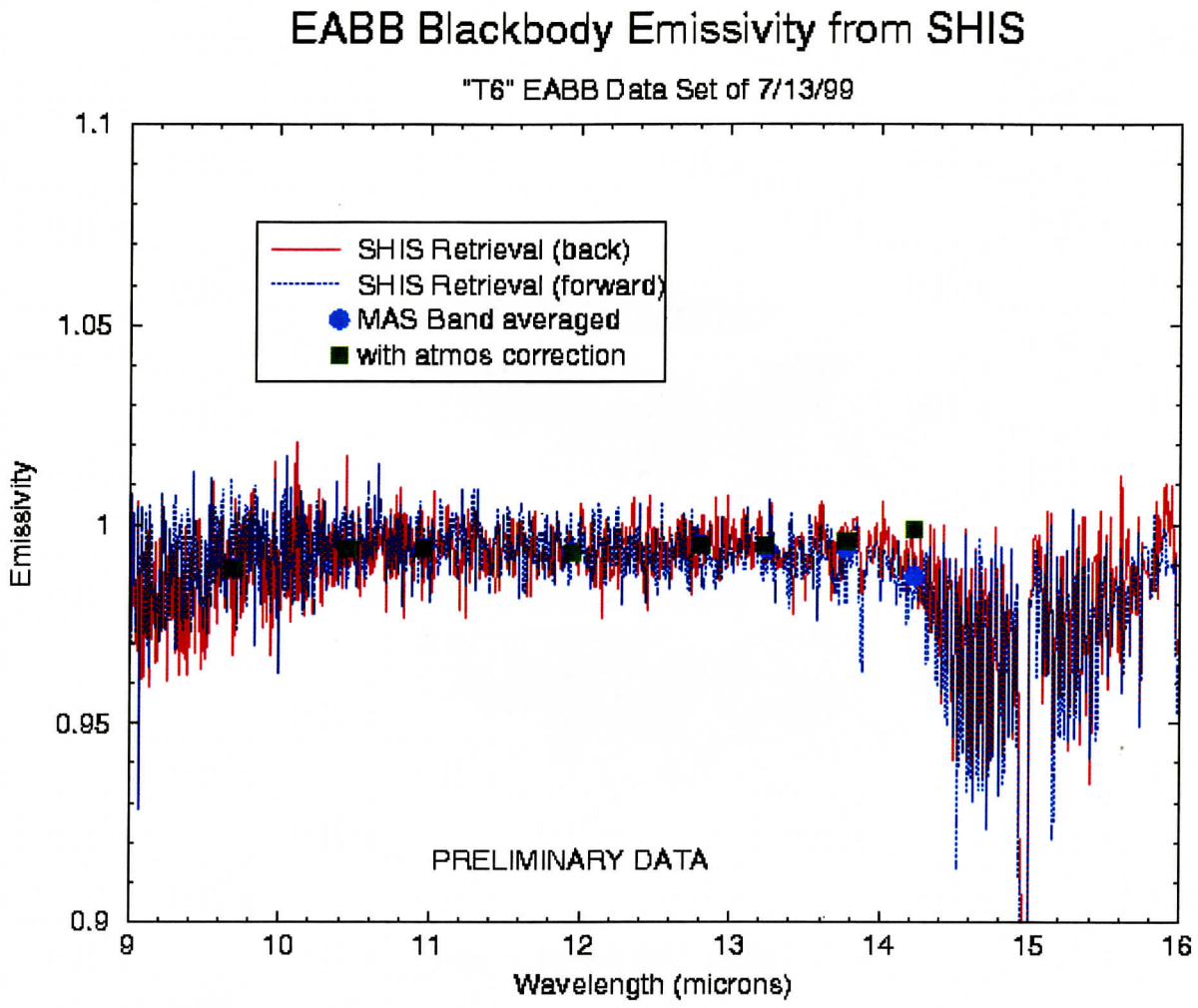

Figure 9. Extended AREA Blackbody (EABB) derived emissivity using S-HIS measurements from July 1999. Green and blue marks represent the emissivity convolved over the MAS spectral response with and without correction for intervening atmospheric absorption . The EABB emissivity is advertised as being > .995 for LWIR wavelengths; the S-HIS emissivity retrievals are close to these values. Importantly the chart demonstrates that the EABB emissivity is approximately uniform across the LWIR spectral range. This eliminates the EABB as the cause of lower than expected 14um effective emissivity estimates from MAS observations of the EABB.